

Control of Current Reversal in Single and Multiparticle Inertia Ratchets

H. A. Larrondo¹, Fereydoon Family², C. M. Arizmendi^{1,2}

¹ *Depto. de Física, Facultad de Ingeniería, Universidad Nacional de Mar del Plata,*
Plata,
Av. J.B. Justo 4302, 7600 Mar del Plata,
Argentina

²*Department of Physics, Emory University, Atlanta, GA 30322, USA*

(October 27, 2018)

Abstract

We have studied the deterministic dynamics of underdamped single and multiparticle ratchets associated with current reversal, as a function of the amplitude of the external driving force. Two experimentally inspired methods are used. In the first method the same initial condition is used for each new value of the amplitude. In the second method the last position and velocity is used as the new initial condition when the amplitude is changed. The two methods are found to be complementary for control of current reversal, because the first one elucidates the existence of different attractors and gives information about their basins of attraction, while the second method, although history dependent, shows the locking process. We show that control of current reversals in deterministic inertia ratchets is possible as a consequence of a locking process associated with different mean velocity attractors. An unlocking effect

is produced when a chaos to order transition limits the control range.
87.15.Aa, 87.15.Vv, 05.60.Cd, 05.45.Ac

Stochastic models known as *thermal ratchets* or *correlation ratchets* [1], in which a nonzero net drift velocity may be obtained from fluctuations interacting with broken symmetry structures [2], have recently received much attention. This interest is due to the possible applications of these models for understanding molecular motors [3], nanoscale friction [4], surface smoothing [5], coupled Josephson junctions [6], optical ratchets and directed motion of laser cooled atoms [7], and mass separation and trapping schemes at the microscale [8]. The fluctuations that produce the net transport are usually associated with noise, but they may arise also in absence of noise, with additive forcing, in overdamped deterministic systems [9], overdamped quenched systems [10] and in underdamped systems [11–14].

Inertial ratchets, even in the absence of noise have a very complex dynamics, including chaotic motion [11,12]. This deterministically induced chaos mimics, to some extent, the role of noise [15], changing, on the other hand, some of the basic properties of thermal ratchets. For example, inertial ratchets can exhibit multiple reversals in the current direction [11,12]. The direction depends on the amount of friction and inertia, which makes it especially interesting for technological applications such as microscopic particle separation [8].

Jung *et al* [11] studied the case of an underdamped particle periodically driven in an asymmetric potential without noise and found multiple current reversals varying with the intensity of the external perturbation. They characterized the motion by cumulants of the contracted, time-dependent solution of the Liouville equation and distinguished regular from chaotic transport.

Several attempts to find the mechanism causing these current inversions have been made. Mateos [12] analyzed the relation between the bifurcation diagram and the current. He conjectured that the origin of the current reversal is the bifurcation from a chaotic to a periodic regime. Close to this bifurcation he observed trajectories revealing intermittent chaos and anomalous deterministic diffusion. Barbi *et al.* [13] related the transport properties to phase locking dynamics. They interpreted the current reversals in terms of different stability properties of the periodic rotating orbits and reported cases where current reversals appear also in the absence of a bifurcation from a chaotic to a periodic motion. Although the

origin of current inversions seems to be relatively clear, this has not been enough to propose a method to control the multiple current reversals which is important technologically.

The aim of this paper is to elucidate the relationship between bifurcation diagrams, phase locked dynamics and transport phenomena for an underdamped deterministic ratchet without noise in order to find a way to control the current reversals.

Specifically we study the dimensionless equation of motion:

$$\epsilon \ddot{x} + \gamma \dot{x} = \cos(x) + \mu \cos(2x) + \Gamma \sin(\omega t). \quad (1)$$

Here, ϵ is the mass of the particle, γ is the damping coefficient, Γ and ω are respectively the amplitude and frequency of an external oscillatory forcing. The asymmetric potential is given by

$$U(x) = -\sin(x) - \frac{\mu}{2} \sin(2x).$$

Numerical solutions of Eq. (1) are obtained using a variable step Runge-Kutta-Fehlberg method [16]. We fixed $\epsilon = 1.1009$, $\gamma = 0.1109$, $\mu = 0.5$ and $\omega = 0.67$ and studied the behavior of the system as a function of Γ . These parameters were chosen because they are in the same region as used by Barbi and Salerno [13].

Let us start analyzing the case of only one particle with a specific initial condition. The values of $x(t)$ and $v(t)$ are sampled with a sampling period $T_s = T/20$ where T is the period of the driving force (i.e. $T = 2\pi/\omega$).

The mean velocity of the particle is defined as:

$$\langle v \rangle = \frac{x(n_{\max}T) - x(n_{\text{tran}}T)}{(n_{\max} - n_{\text{tran}})T},$$

where the number of periods of the transitory was chosen as $n_{\text{tran}}=400$ and the average was done until $n_{\max}=500$ periods.

There are at least two different ways to do a real experiment to study the effect of the variation of the strength of the external force Γ . One way is to let the particle evolve starting from the same initial condition when Γ changes. Another possible way is to change

Γ in the middle of the trajectory of the particle. Simulations were carried out with both methods, that will be called method I and II respectively, corresponding to the two possible experimental realizations.

Let us first present the results of method I. The normalized mean velocity $\langle v \rangle / v_\omega$, with $v_\omega = T_x/T$, where T_x is the spatial period of the potential is shown in figure 1a for a particle with initial condition ($x_0=0, v_0=1$) as a function of the amplitude of the external oscillatory forcing Γ . The simulation was done by resetting the initial condition to the same values ($x_0=0, v_0=1$) when Γ was changed. The corresponding bifurcation diagram is plotted in figure 1b. Figures 1c and 1d are enlargements for $\Gamma \in [1, 1.05]$. There are several important remarks concerning these figures: a) there exist several inversions in $\langle v \rangle$ inside regions of the same locking characteristics, which means regions where v is periodic with the same period commensurate with T , (see for example four of such inversions in Γ between 1.01 and 1.015); b) there are regions of different locking characteristics and the same mean velocity (see for example the region with Γ between 1.015 and 1.035 and the region near $\Gamma=1.045$); c) the values of Γ where the inversions in $\langle v \rangle$ take place are strongly dependent on initial conditions.

To understand these characteristics, the trajectories are shown in figures 2 to 4. In figures 2a and 2b we show the case of two trajectories corresponding to different locking zones ($\Gamma=1.015$ and $\Gamma=1.035$). Both trajectories (2a and 2b) show the same net transport given by a straight line with slope $\langle v \rangle = v_\omega$ but the oscillations \tilde{x} over this straight line are different as can be seen in figures 2c and 2d where the phase spaces $(\tilde{x}/T_x, v/v_\omega)$ are shown.

In figure 3 the case of a mean velocity reversal inside the period-1 zone is shown; the complete trajectories for $\Gamma=1.01$ and $\Gamma=1.011$ are drawn in 3a and 3b respectively. In 3c and 3d we show the transitory with greater detail.

Finally in figure 4 the case $\Gamma=1.527$ corresponding to chaotic motion is analyzed. In figure 4a we have plotted the trajectory $x(t)$ showing clearly that we are in the presence of a net-transport phenomenon and in 4b we show the phase space with the chaotic oscillations

superimposed.

The above results clearly show that with method I the bifurcation diagram gives the behavior of the oscillations superimposed on the mean motion and not the net-transport movement. The phase locking analysis is a useful tool for the study of the synchronization between auto-oscillatory systems with an external periodic driving force [17]. In that case the variables x and v are both periodic (i.e. S^1) and the net transport is automatically discarded.

Figs. 5 and 6 show the normalized mean velocity and the bifurcation diagram obtained with method II, which means taking last position and velocity of the trajectory of the previous Γ as the initial condition for the new Γ . The step $\Delta\Gamma$ is 0.001 and the particle evolves during $499T$ for each Γ . Fig. 5 was obtained beginning with $\Gamma=0.89665$ as the initial Γ . The normalized mean velocity remains unchanged equal to 1 until Γ approximately 1.05. Fig. 6 was obtained beginning with $\Gamma=0.89666$ as the initial Γ . The normalized mean velocity remains unchanged at -1 until Γ is approximately 1.08. The initial Γ was chosen so that there is a current reversal between them as can be seen in Fig. 1 c). In Figs. 5a) and 6a) there is no current reversal in the range $[0.9, 1.05]$, while there are many current reversals in the same zone of Fig. 1 a). On the other hand, the bifurcation diagrams of Figs. 5b) and 6b) are continuous but different from each other, furthermore none of them shows the abrupt changes appearing in the same zone of Fig. 1b).

These results may be explained if there are two attractors corresponding to mean velocities $+v_\omega$ and $-v_\omega$. In each of the simulations obtained by method II the particle remains locked into one of the attractors. The current reversals of Fig. 1 are due to the fact that the border between the basins of attraction changes with Γ . For Γ in some region around $\Gamma=1$ the mean velocity may be positive or negative depending on which basin of attraction the initial condition belongs to. This sensitivity to the initial condition may be used to control current reversals by means of a small perturbation in Γ when the particle is near the border of a basin of attraction. An experiment may be envisioned where a digital generator is used as the external force, in that case the step in Γ and the precise time when the change is

applied may be tuned to control the trajectory of each particle. As an example in Fig. 7 we show the case of a particle starting at $x_0=0$ and $v_0=1$ with $\Gamma = 0.89665$. This particle reaches a final value of $\langle v \rangle / v_\omega=1$ as can be seen in Fig. 1. The bold curve in Fig. 7 shows the effect of changing Γ to 0.89675 at time $t = 498.7T$, when the particle is at $x = 3.1097 + 2n\pi$ with an instantaneous velocity $v = 0.911662$. Due to this change, movement of the particle is reversed. On the contrary, if the same change in Γ is produced at $t = 499T$, when the particle is at $x = 1.0597 + 2n\pi$ with an instantaneous velocity $v = -1.82108$, the inversion does not occur as is shown with the thin curve.

These above results were obtained by studying the trajectory of only one particle, but ratchet transport is essentially stochastic. This was already pointed out by Feynman [18], when he used the ratchet to introduce the Second Law of Thermodynamics. In deterministic inertial ratchets deterministically induced chaos mimics the role of noise [15] and this calls for the use of a time dependent probability measure, as has been previously done in [11,10,14].

We use a collection of particles with different initial conditions to study the transport phenomena. We work with an ensemble of N particles having identical initial velocities v_0 but initial positions equally distributed in the range $[x_{\min}, x_{\max}]$. The initial probability density is given by:

$$\rho(x, v, 0) = \delta(v - v_0) [H(x - x_{\min}) - H(x - x_{\max})],$$

where $H(x)$ is the step function.

The normalized mean-velocity of the ensemble is:

$$\langle\langle V \rangle\rangle = \frac{1}{N} \sum_{i=1}^N \langle v \rangle_i .$$

As for the one particle case we first show the results of simulations with method I, which in the packet of particles means returning to the initial condition $\rho(x, v, 0)$ when Γ changes.

The results shown in figure 8 were obtained with $N=200$ and $[x_{\min}, x_{\max}] = [5.08, 11.35]$ and $v_0 = 0.01$ corresponding to a well spread-out packet of particles with initial positions between two maxima of the potential. The corresponding bifurcation diagram is also shown.

There is only one current reversal at $\Gamma \simeq 1.05$, where an order-disorder transition takes place. About three quarters of the particles in the ensemble have mean velocity $\langle v \rangle_i = -v_w$ and the remaining quarter have $\langle v \rangle_i = v_w$ giving a normalized ensemble mean velocity $\langle\langle V \rangle\rangle / v_w \simeq -0.5$. These results seem to agree with Mateos' conjecture [12] that current inversion is associated with order-disorder transition in the bifurcation diagram.

In order to obtain the behavior corresponding to a narrow initial packet, we work with the initial condition $[x_{\min}, x_{\max}] = [5.08, 5.09]$ and $v_0 = 0.01$. In this ensemble particles are initially located near the maximum of the potential and having a small initial velocity. Fig. 9 shows a current inversion around $\Gamma = 1.015$. The corresponding region at the bifurcation diagram has no order-disorder transition, contradicting Mateos' conjecture. However, the same current reversal, associated with an order-disorder transition, which was obtained for the case of a wide packet for $\Gamma \simeq 1.05$, does take place.

Initial sets of particles with positions near the minimum of the potential and sets of particles with identical initial positions and different initial velocities equally distributed were also studied with qualitatively similar results.

It is possible to use method II to control the normalized mean velocity of the packet. For example to obtain a normalized mean velocity $\langle\langle V \rangle\rangle / v_w = -0.5$ which is the minimum normalized mean velocity of Fig. 9 a), with the same narrow packet used above we use method II starting with $\Gamma_{\min} = 1.013$ and increasing it up to $\Gamma = 1.06$ in 100 equal steps. The time period for each step in Γ was commensurate with T . The normalized mean velocity as a function of Γ is shown in Fig. 10 a). The corresponding bifurcation diagram is shown in Fig. 10b). As Γ changes each particle remains locked to its mean velocity $\langle v \rangle_i$ corresponding to Γ_{\min} and the packet also remains locked to its initial mean velocity. This behavior persists until $\Gamma = 1.0495$ where the mean velocity drops to $\langle\langle V \rangle\rangle / v_w = -1$. The unlocking effect corresponds to a chaos to order transition. If the simulation starts with any Γ_{\min} producing a positive velocity locking for the packet the unlocking effect produces a current reversal as Mateos found.

In summary, we studied the variation of the mean velocity of one particle and of a packet

of particles with the amplitude of the external force Γ in two ways. The first one consists of returning to the initial conditions whenever Γ is changed. In this way many current reversals appear which are not associated with the bifurcations in the bifurcation diagram. The second way is to take as initial condition the last position and velocity of the previous trajectory for a given Γ . When this method is used, the mean velocity remains locked in the periodic zones of the bifurcation diagram. The differences between the results obtained with both methods may be explained by the presence of at least two attractors associated with positive and negative mean velocities. The two methods are complementary as possible mechanisms for the control of current reversal, because method I reveals the existence of different attractors and gives information about their basins of attraction, while method II, although history dependent, shows the locking process.

We conclude that control of current reversals in deterministic inertial ratchets is possible as a consequence of a locking process associated with different mean velocity attractors. An unlocking effect is produced when a chaos to order transition limits the control range.

This work was supported by grants from the Office of Naval Research and from the Universidad Nacional de Mar del Plata. We acknowledge Mihail N. Popescu for very useful discussions on simulation methods and control. C.M.A. acknowledges Alvaro L. Salas Brito for useful discussions.

REFERENCES

- [1] C.R. Doering, *Il Nuovo Cimento* **17**, 685 (1995); P. Hänggi and R. Bartussek, *Lecture Notes in Physics*, edited by J. Parisi, S.C. Müller, and W. Zimmerman (Springer, Berlin, 1996), Vol. 476, pp. 294-308; R.D. Astumian, *Science* **276**, 917 (1997).
- [2] A. Ajdari and J. Prost, *C. R. Acad. Sci. Paris* **315**, 1635 (1992); M. O. Magnasco, *Phys. Rev. Lett.* **71**, 1477 (1993).
- [3] N. J. Córdova, B. Ermentrout, and G. Oster, *Proc. Natl. Acad. Sci.* **89**, 339 (1992); J. Maddox, *Nature (London)* **365**, 203 (1993); **368**, 287 (1994); **369**, 181 (1994); S. Leibler, *ibid.* **370**, 412 (1994); R. D. Astumian and M. Bier, *Phys. Rev. Lett.* **72**, 1766 (1994); C. R. Doering, B. Ermentrout and G. Oster, *Biophys. J.* **69**, 2256 (1995); R. D. Astumian and I. Derényi, *Eur. Biophys. J.* **27**, 474 (1998).
- [4] J. Krim, D. H. Solina and R. Chiarello, *Phys. Rev. Lett.* **66**, 181 (1991); J. B. Sokoloff, J. Krim and A. Widom, *Phys. Rev. B* **48**, 9134 (1993); L. Daikhin and M. Urbakh, *Phys. Rev. E* **49**, 1424 (1994); C. Daly and J. Krim, *Phys. Rev. Lett.* **76**, 803 (1996); M. R. Sorensen, K. W. Jacobseen and P. Sstoltze, *Phys. Rev. B* **53**, 2101 (1996).
- [5] I. Derényi, Choongseop Lee and Albert-László Barabási, *Phys. Rev. Lett.* **80**, 1473 (1998). Albert-László Barabási and H. E. Stanley, *Fractal Concepts in Surface Growth* (Cambridge University Press, Cambridge, UK, 1995).
- [6] I. Zapata, R. Bartussek, E. Sols and P. Hänggi, *Phys. Rev. Lett.* **77**, 2292 (1996).
- [7] L. P. Faucheux, L. S. Bbourdieu, P. D. Kaplan and A. J. Libchaber, *Phys. Rev. Lett.* **74**, 1504 (1995); C. Mennerat-Robilliard *et al.* *Phys. Rev. Lett.* **82**, 851 (1999).
- [8] A. Adjari, D. Mukamel, L. Peliti, and J. Prost, *J. Phys. I (France)* **4**, 1551 (1994); L. Gorre-Talini, J. P. Sspatz, and P. Silberzan, *Chaos* **8**, 650 (1998); I. Derényi and R. D. Astumian, *Phys. Rev. E* **58**, 7781 (1998); D. Ertas, *Phys. Rev. Lett.* **80**, 1548 (1998); T. A. J. Duke and R. H. Austin, *Phys. Rev. Lett.* **80**, 1552 (1998).

- [9] P. Hänggi and R. Bartussek, *Lecture Notes in Physics*, edited by J. Parisi, S.C. Müller, and W. Zimmerman (Springer, Berlin, 1996), Vol. 476; J. F. Chauwin, A. Adjari, and J. Prost, *Europhys. Lett.* **27**, 421 (1994); J. F. Chauwin, A. Adjari, and J. Prost, *Europhys. Lett.* **32**, 373 (1995).
- [10] M. N. Popescu, C. M. Arizmendi, A. L. Salas-Brito and F. Family, *Phys. Rev. Lett.* **85**, 3321-3324 (2000)
- [11] P. Jung, J. G. Kissner and P. Hänggi. *Phys. Rev. Lett.* **76**, 3436-3439 (1996).
- [12] J. L. Mateos, *Phys. Rev. Lett.* **84**, 258-261 (2000).
- [13] M. Barbi and M. Salerno, *Phys. Rev. E* **62**, 1988-1994, (2000).
- [14] C. M. Arizmendi, F. Family and A. L. Salas-Brito, *Phys. Rev. E* **63** 061104 (2001).
- [15] A nice study that uses deterministic chaos instead of noise in a ratchet is T. Hondou and Y. Sawada, *Phys. Rev. Lett.* **75**, 3269 (1995)
- [16] W. H. Press, S. A. Teikolsky, W. T. Vetterling, and B. P. Flannery, *Numerical Recipes in C*, (Cambridge University Press, Cambridge, 1995), pp. 704-716.
- [17] M. Lakshmanan and K. Murali, *Chaos in Nonlinear Oscillators - Controlling and Synchronization* (World Scientific, Singapore, 1996).
- [18] R. P. Feynman, R. B. Leighton, and M. Sands, *The Feynman Lectures on Physics* (Addison-Wesley, Reading, MA, 1966), Vol. 1.

FIGURES

FIG. 1. a) Normalized mean velocity of a particle with initial condition $x_0 = 0, v_0 = 1$ as a function of Γ . Initial condition is reset whenever Γ changes (Method I). b) Velocity bifurcation diagram for a particle with initial condition $x_0 = 0, v_0 = 1$ as a function of Γ . Initial condition is reset whenever Γ changes (Method I). c) Enlargement of Fig. 1a) for Γ between $[1, 1.05]$ d) Enlargement of Fig. 1b) for Γ between $[1, 1.05]$

FIG. 2. a) Trajectory of a particle with initial condition $x_0 = 0, v_0 = 1$ for $\Gamma = 1.015$ b) Trajectory of a particle with initial condition $x_0 = 0, v_0 = 1$ for $\Gamma = 1.035$ c) Phase Space corresponding to oscillations superimposed on the net motion of a particle with initial condition $x_0 = 0, v_0 = 1$ for $\Gamma = 1.015$ d) Phase Space corresponding to oscillations superimposed on the net motion of a particle with initial condition $x_0 = 0, v_0 = 1$ for $\Gamma = 1.035$

FIG. 3. a) Trajectory of a particle with initial condition $x_0 = 0, v_0 = 1$ for $\Gamma = 1.010$ b) Trajectory of a particle with initial condition $x_0 = 0, v_0 = 1$ for $\Gamma = 1.011$ c) Enlargement of the transitory corresponding to the trajectory of a particle with initial condition $x_0 = 0, v_0 = 1$ for $\Gamma = 1.010$ d) Enlargement of the transitory corresponding to the trajectory of a particle with initial condition $x_0 = 0, v_0 = 1$ for $\Gamma = 1.011$

FIG. 4. a) Trajectory of a particle with initial condition $x_0 = 0, v_0 = 1$ for $\Gamma = 1.527$ b) Phase Space corresponding to oscillations superimposed to the net motion of a particle with initial condition $x_0 = 0, v_0 = 1$ for $\Gamma = 1.527$

FIG. 5. a) Normalized mean velocity of a particle with initial condition $x_0 = 0, v_0 = 1$ as a function of Γ starting at $\Gamma = 0.89665$. The initial condition for a given Γ is the last position and velocity of the trajectory of the previous Γ (Method II). b) Velocity bifurcation diagram for a particle with initial condition $x_0 = 0, v_0 = 1$ as a function of Γ starting at $\Gamma = 0.89665$. The initial condition for a given Γ is the last position and velocity of the trajectory of the previous Γ (Method II).

FIG. 6. a) Normalized mean velocity of a particle with initial condition $x_0 = 0, v_0 = 1$ as a function of Γ starting at $\Gamma = 0.89666$. The initial condition for a given Γ is the last position and velocity of the trajectory of the previous Γ (Method II). b) Velocity bifurcation diagram for a particle with initial condition $x_0 = 0, v_0 = 1$ as a function of Γ starting at $\Gamma = 0.89666$. The initial condition for a given Γ is the last position and velocity of the trajectory of the previous Γ (Method II).

FIG. 7. Example of control of current direction by selecting the time when Γ is changed from $\Gamma = 0.89665$ to $\Gamma = 0.89666$. The bold curve corresponds to a changing time $t = 498.7T$. The thin curve corresponds to a changing time $t = 499T$.

FIG. 8. a) Mean velocity of a set of particles with initial positions between two maxima of the potential $[5.08, 11.35]$ and initial velocity $v_0 = 0.01$ as a function of Γ . Initial conditions are reset whenever Γ changes (Method I). b) Velocity bifurcation diagram for a particle of the set of particles with initial positions between two maxima of the potential $[5.08, 11.35]$ and initial velocity $v_0 = 0.01$ as a function of Γ . Initial conditions are reset whenever Γ changes (Method I).

FIG. 9. a) Mean velocity of a narrow set of particles centered at the maximum of the potential and initial velocity $v_0 = 0.01$ as a function of Γ . Initial conditions are reset whenever Γ changes (Method I). b) Velocity bifurcation diagram for a particle of the set of particles centered at the maximum of the potential and initial velocity $v_0 = 0.01$ as a function of Γ . Initial conditions are reset whenever Γ changes (Method I).

FIG. 10. a) Example of control of mean velocity for a narrow distribution of particles centered at the maximum of the potential and initial velocity $v_0 = 0.01$ as a function of Γ starting at $\Gamma = 1.013$. The initial conditions for a given Γ are the last positions and velocities of the trajectories of the previous Γ (Method II). b) Velocity bifurcation diagram for a particle of the set of particles centered at the maximum of the potential and initial velocity $v_0 = 0.01$ as a function of Γ starting at $\Gamma = 1.013$. The initial conditions for a given Γ are the last positions and velocities of the trajectories of the previous Γ (Method II).

Fig. 1

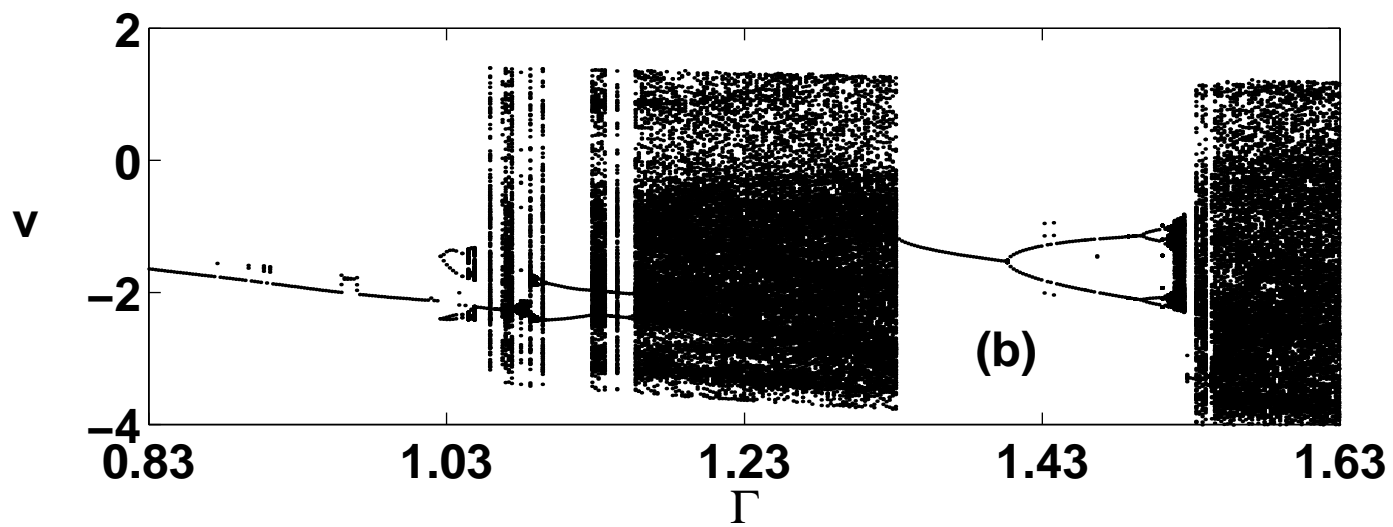
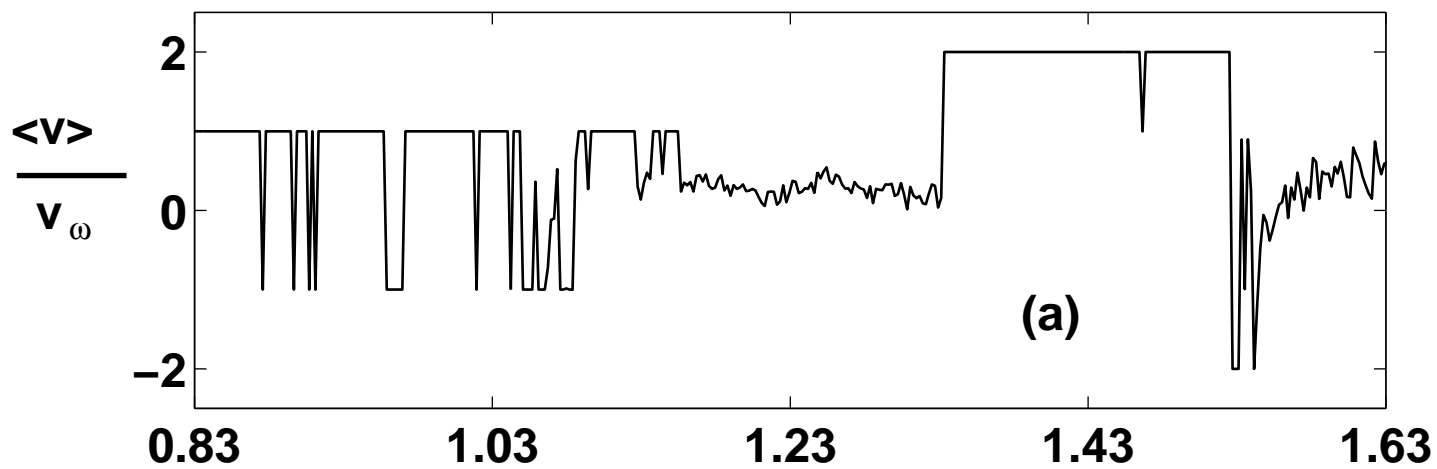


Fig. 1

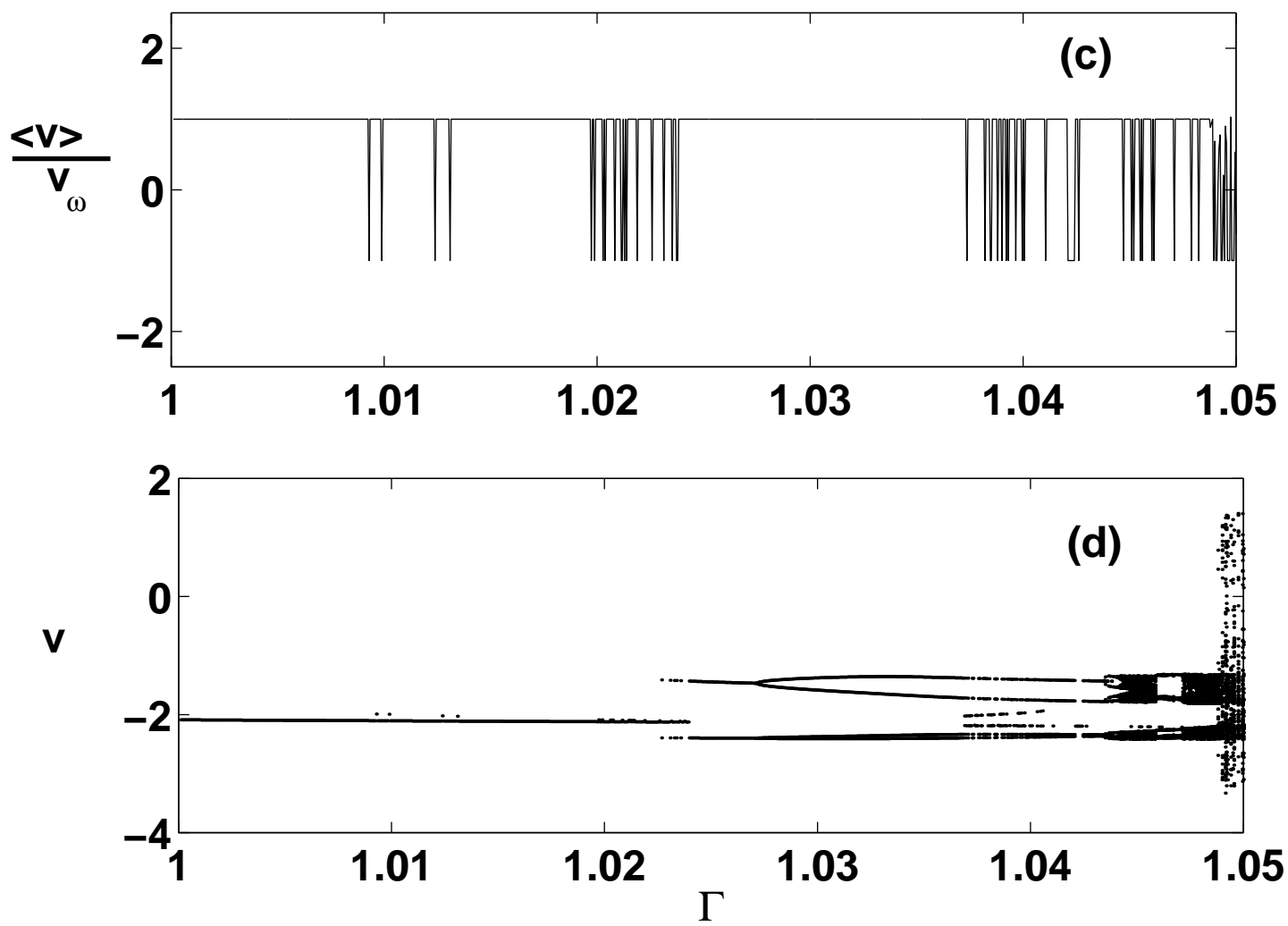


Fig. 2a

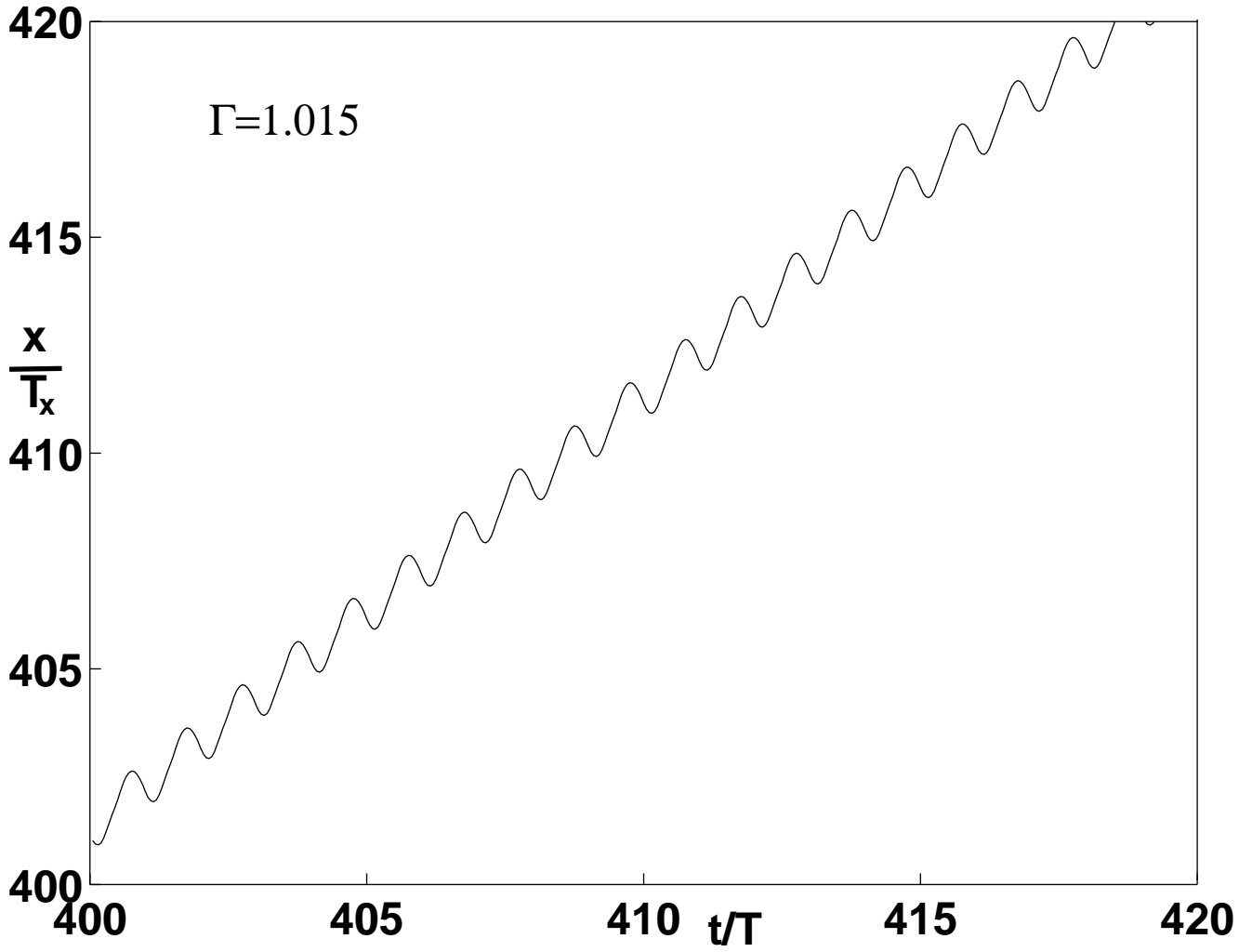


Fig. 2b

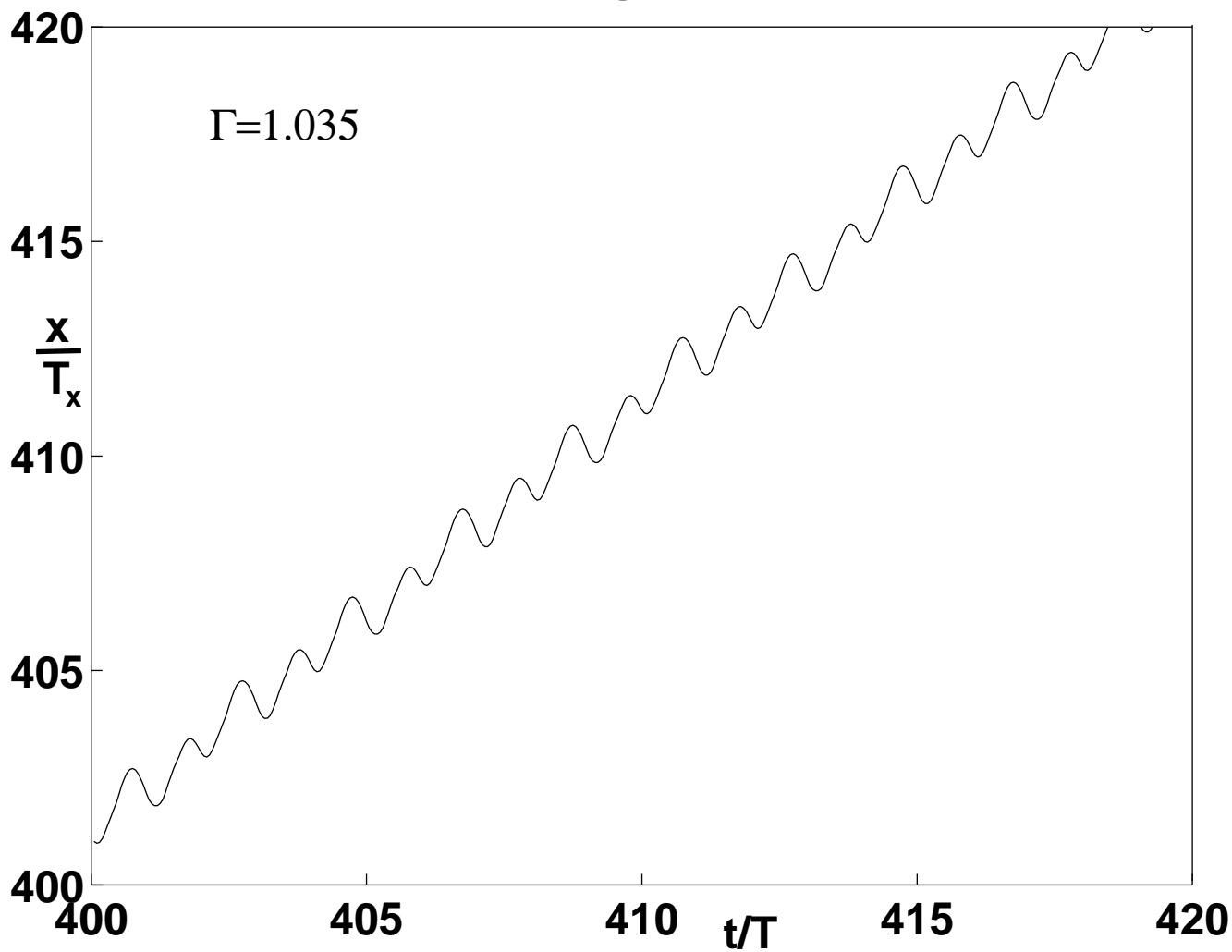


Fig. 2c

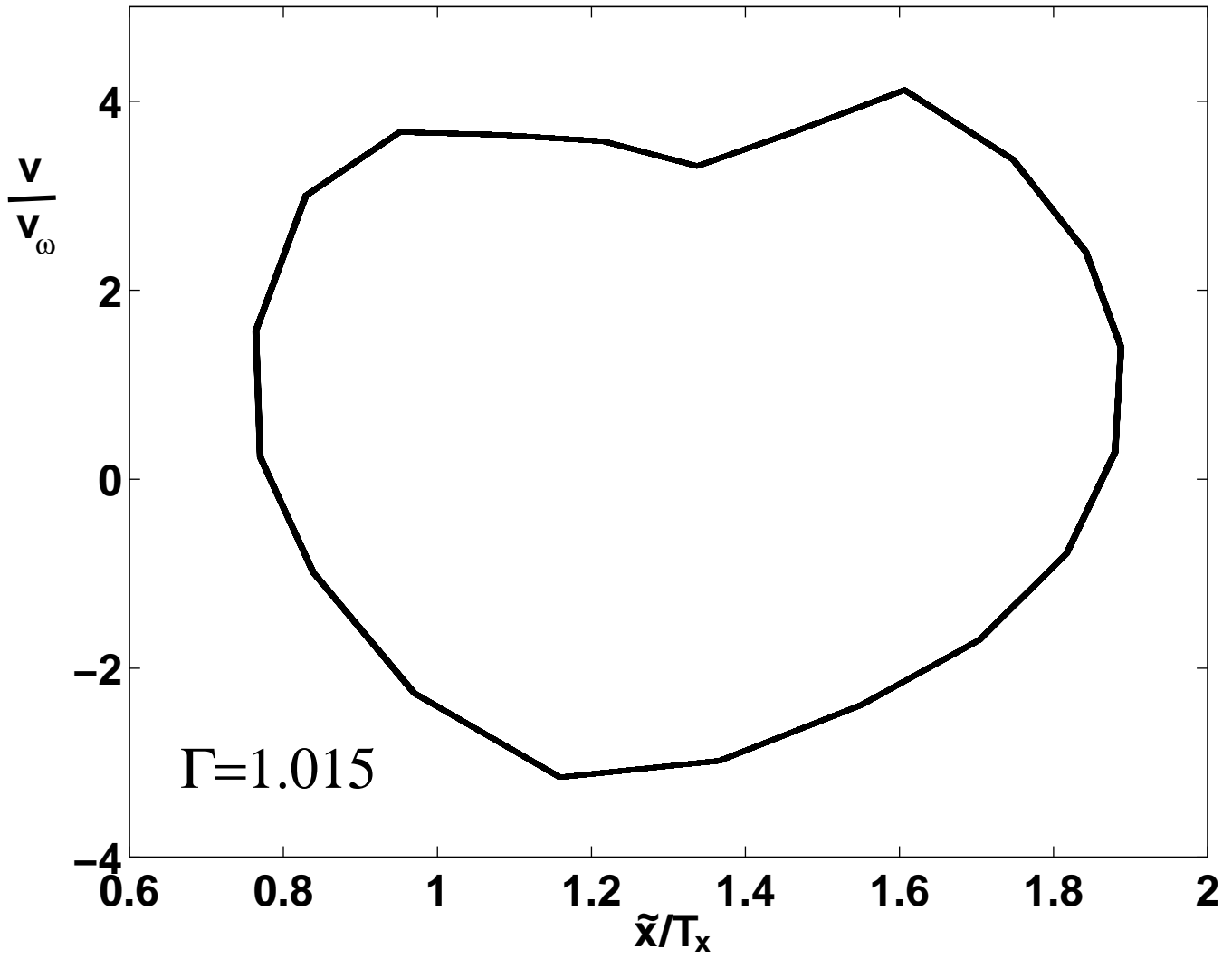


Fig. 2d

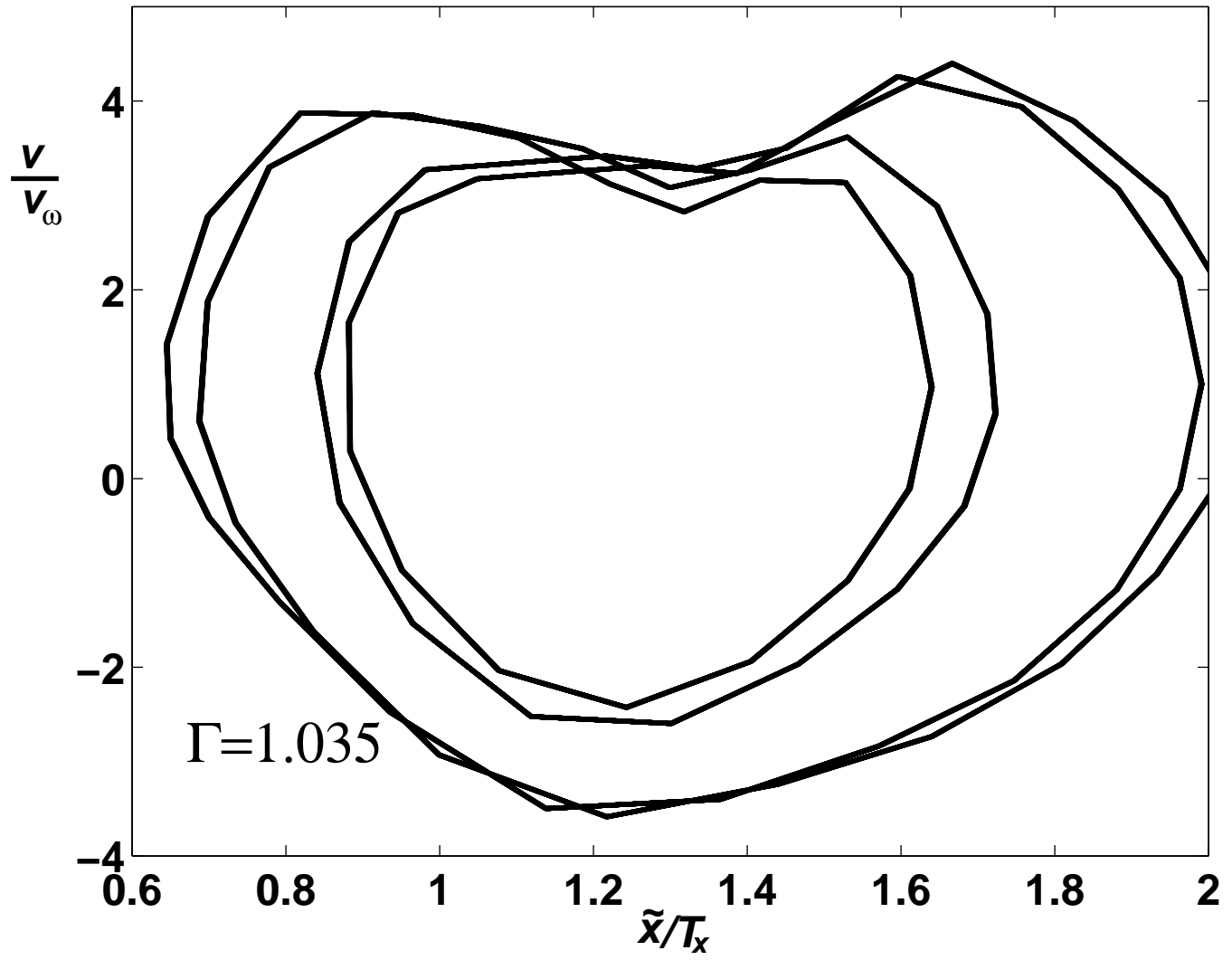


Fig. 3a

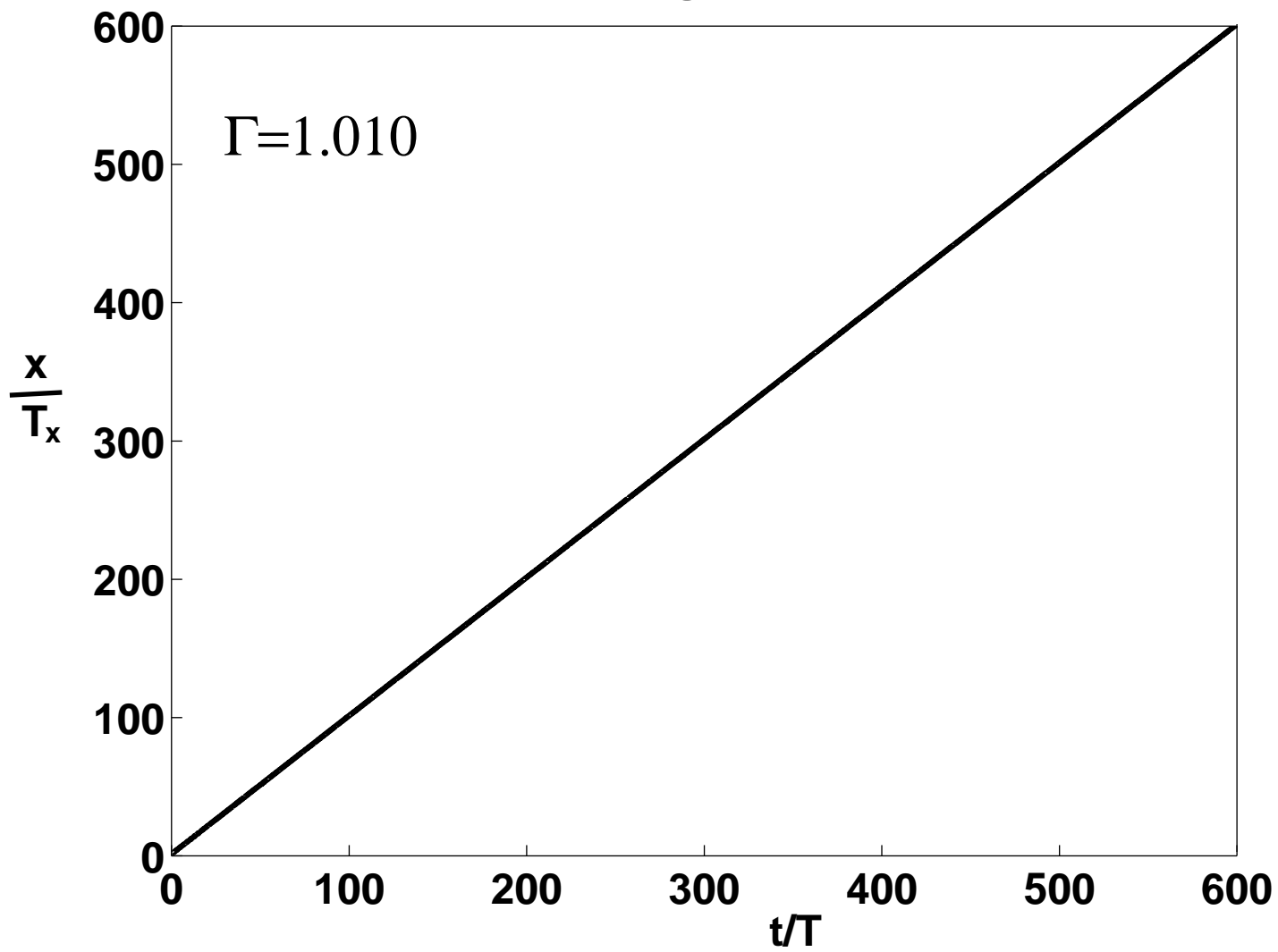


Fig. 3b

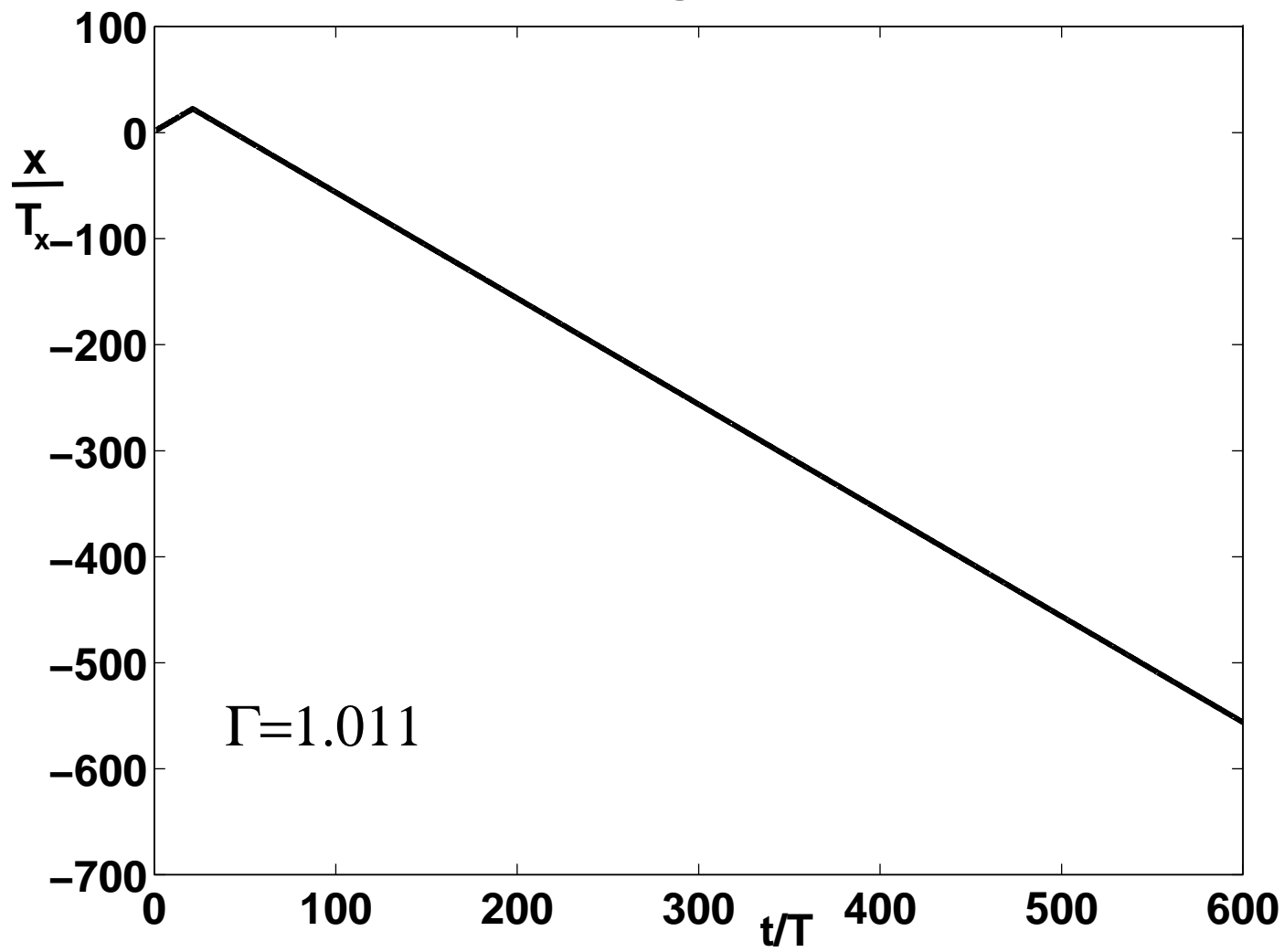


Fig. 3c

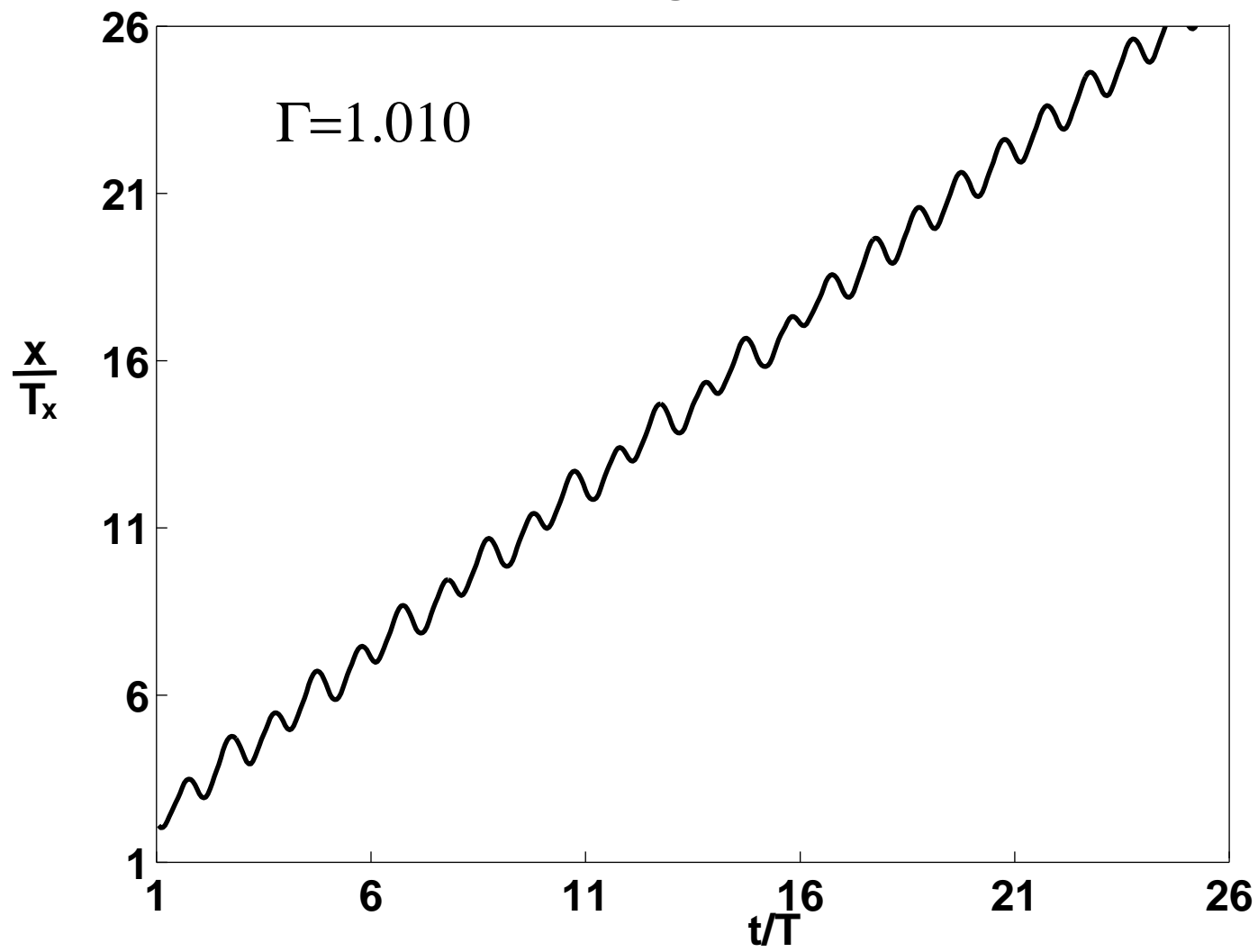


Fig. 3d

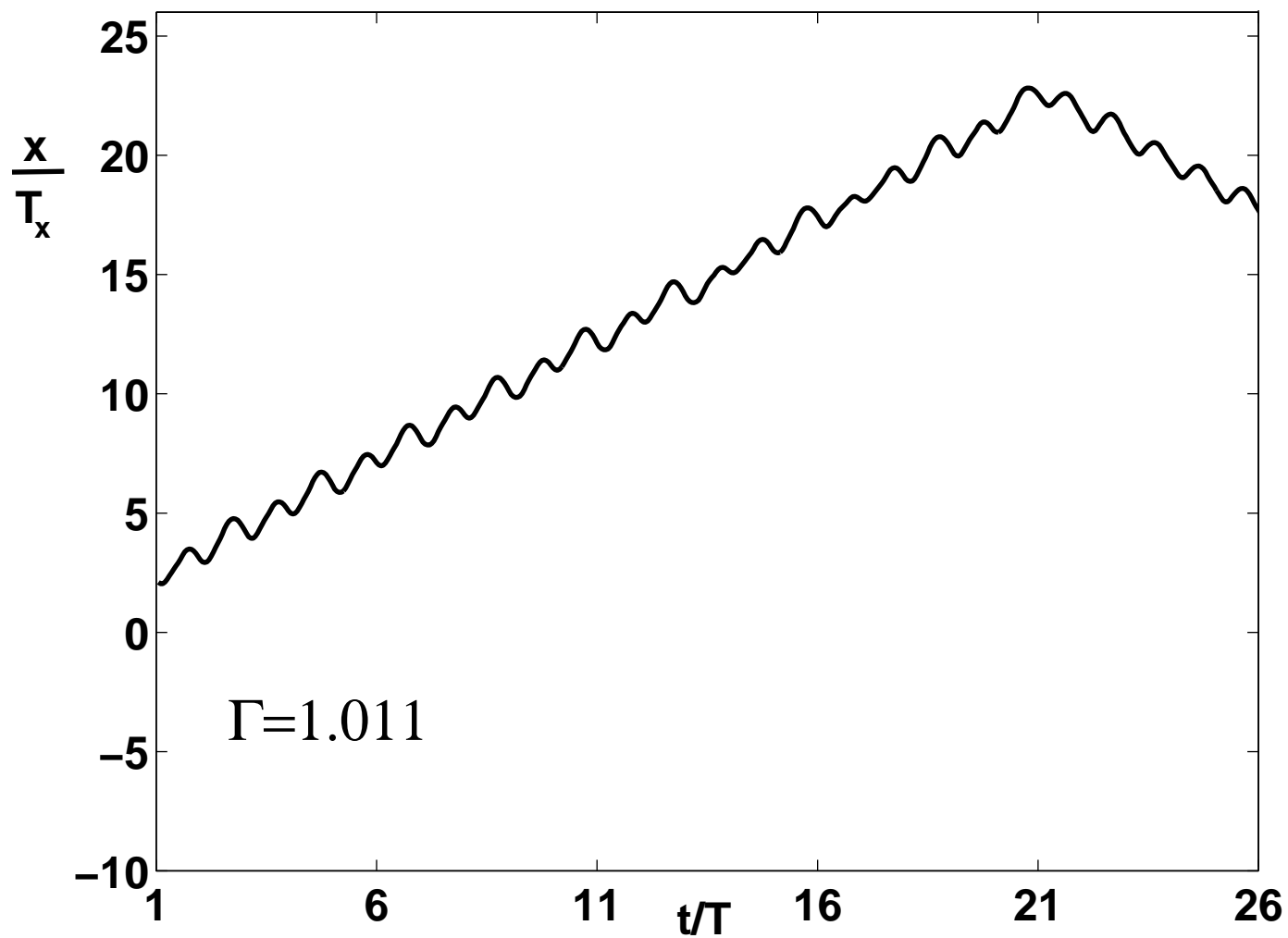


Fig. 4a

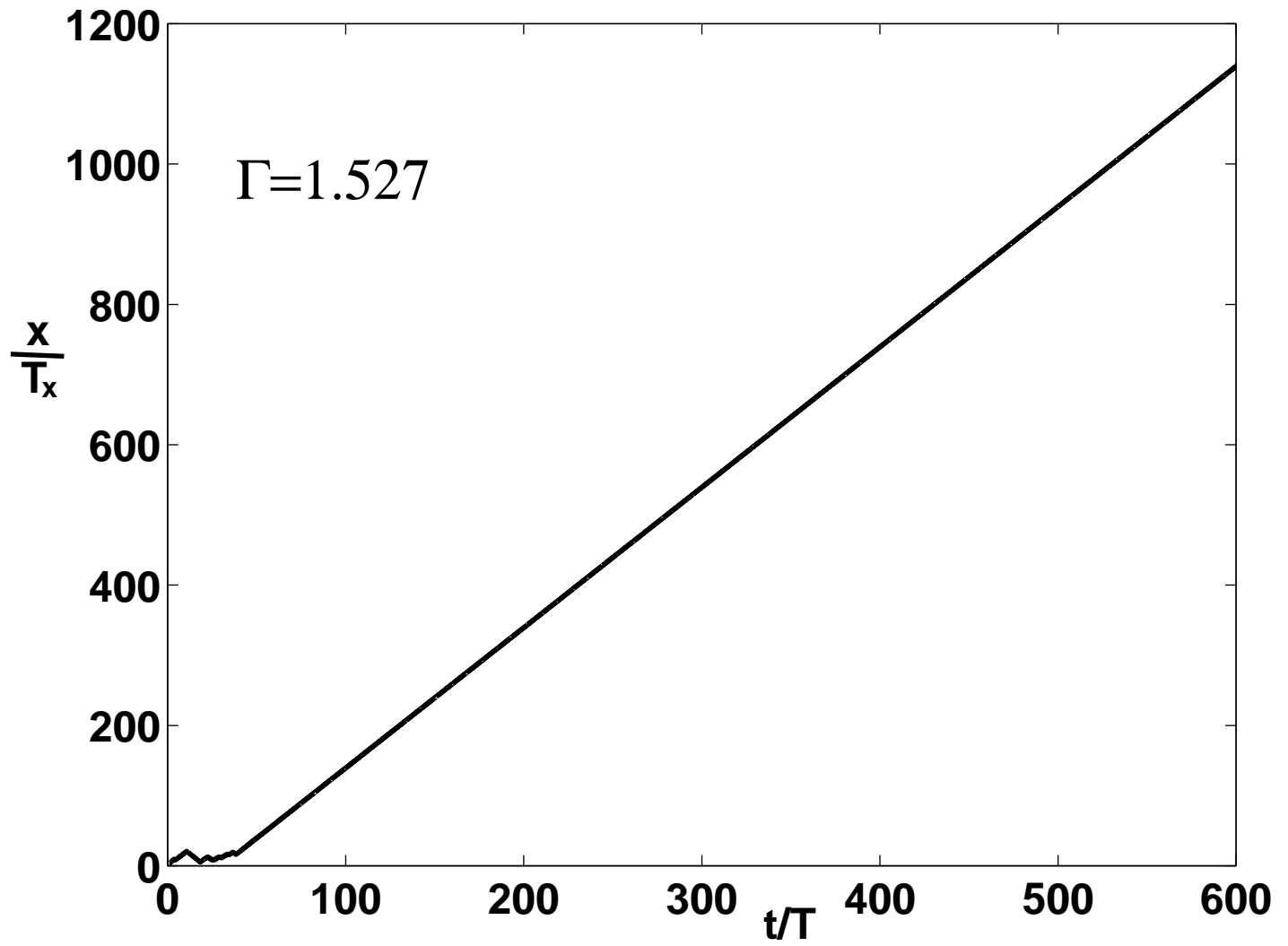


Fig. 4b

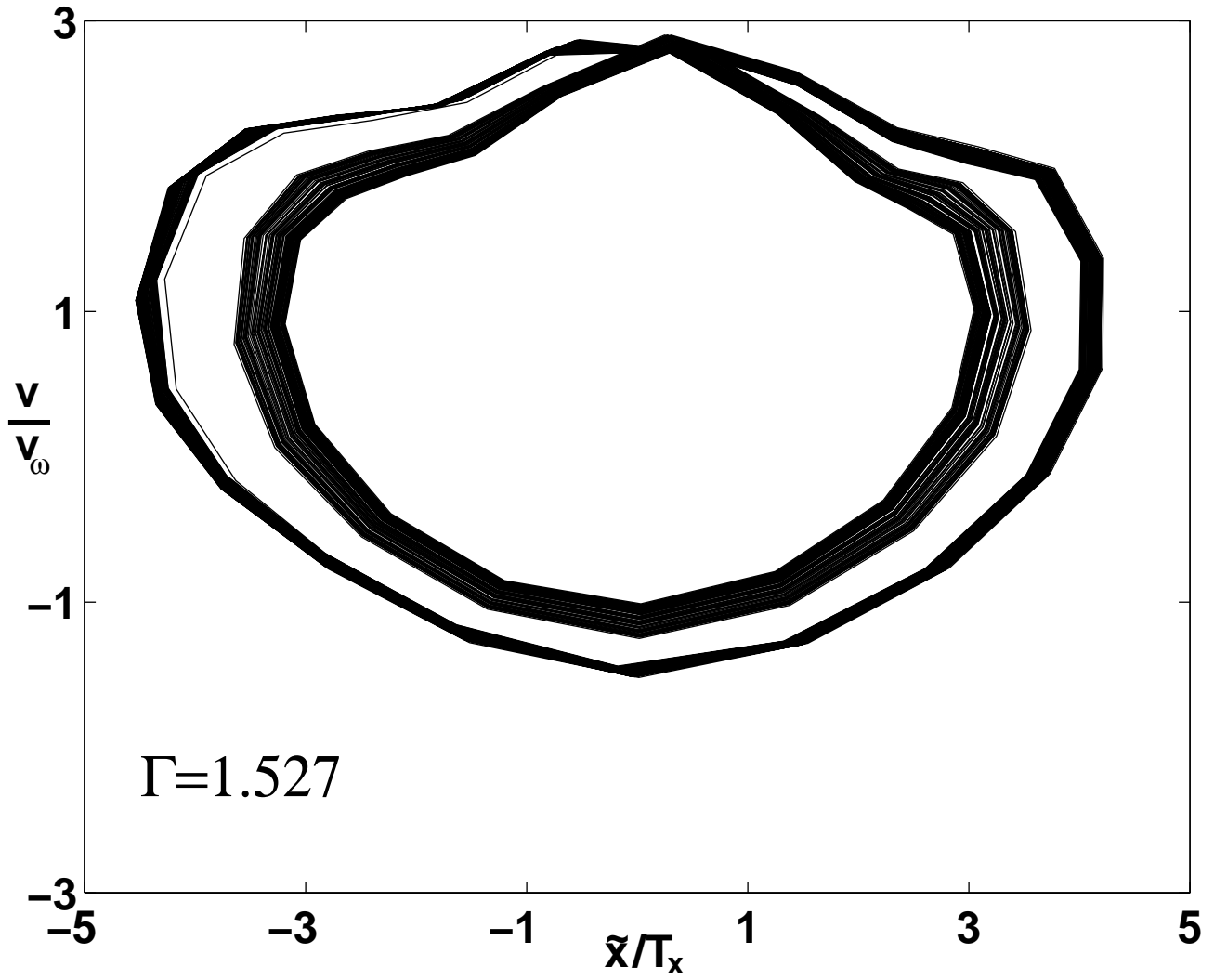


Fig. 5

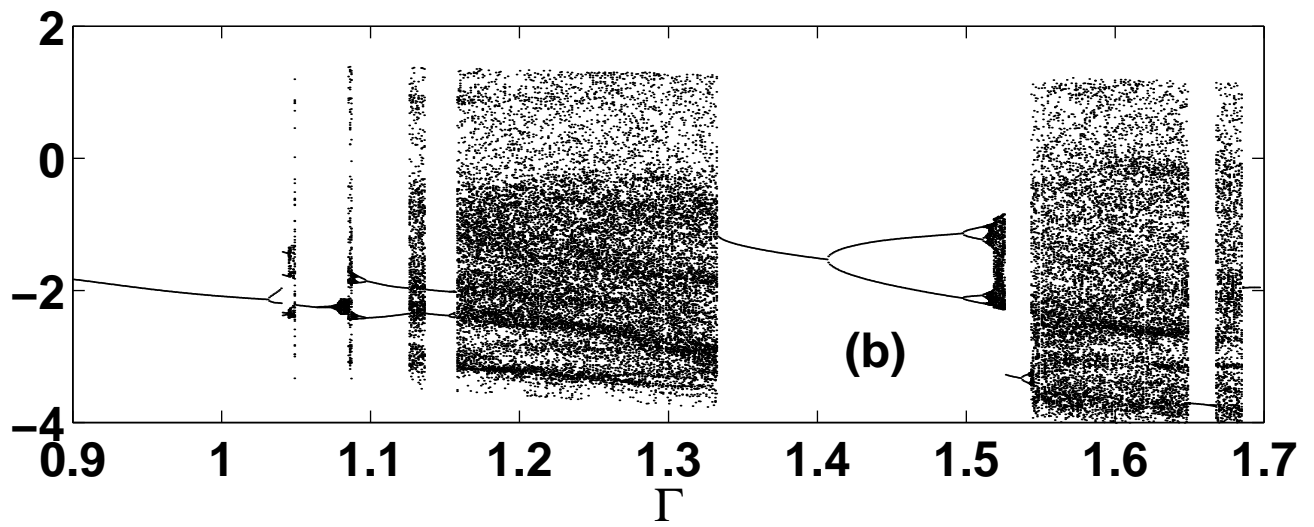
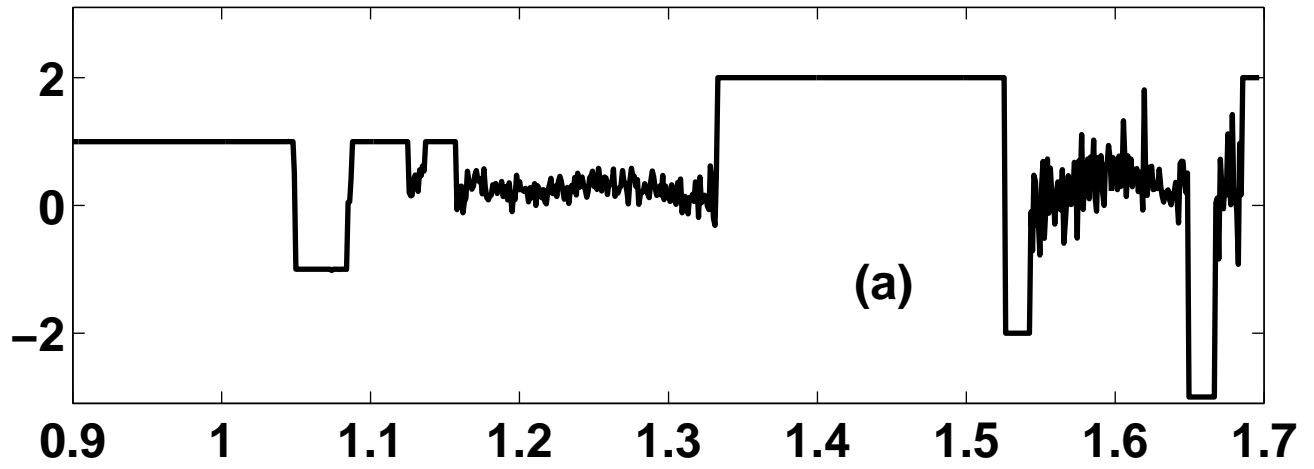


Fig. 6

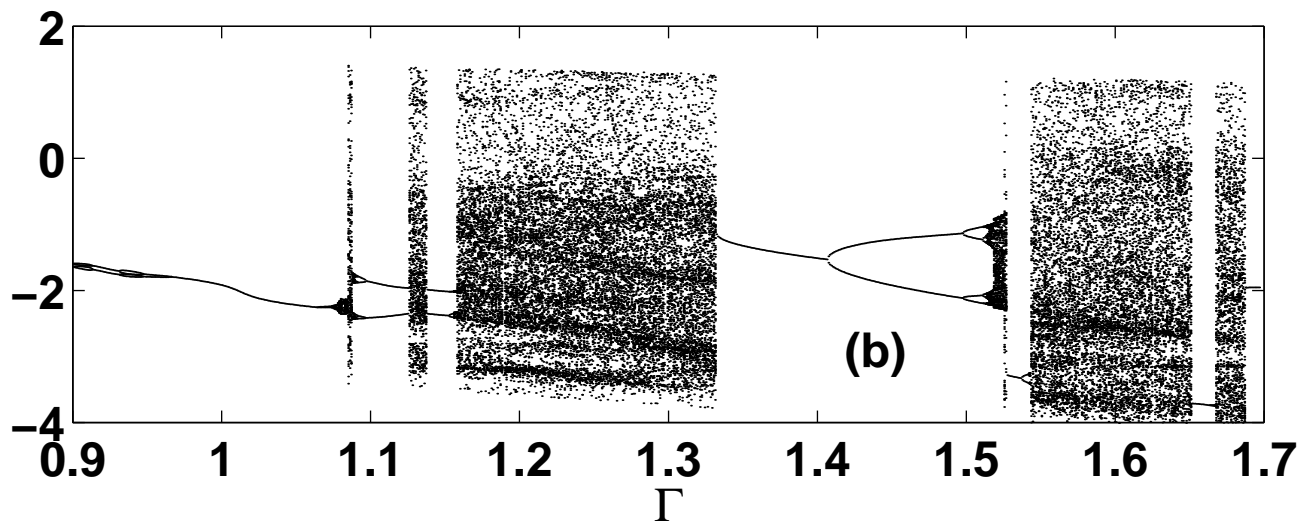
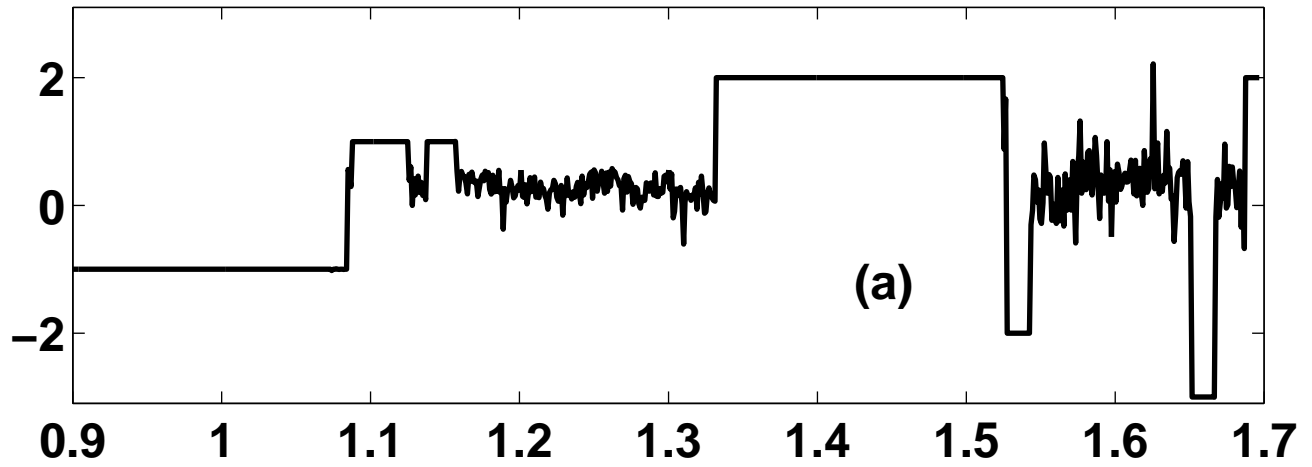


Fig. 7

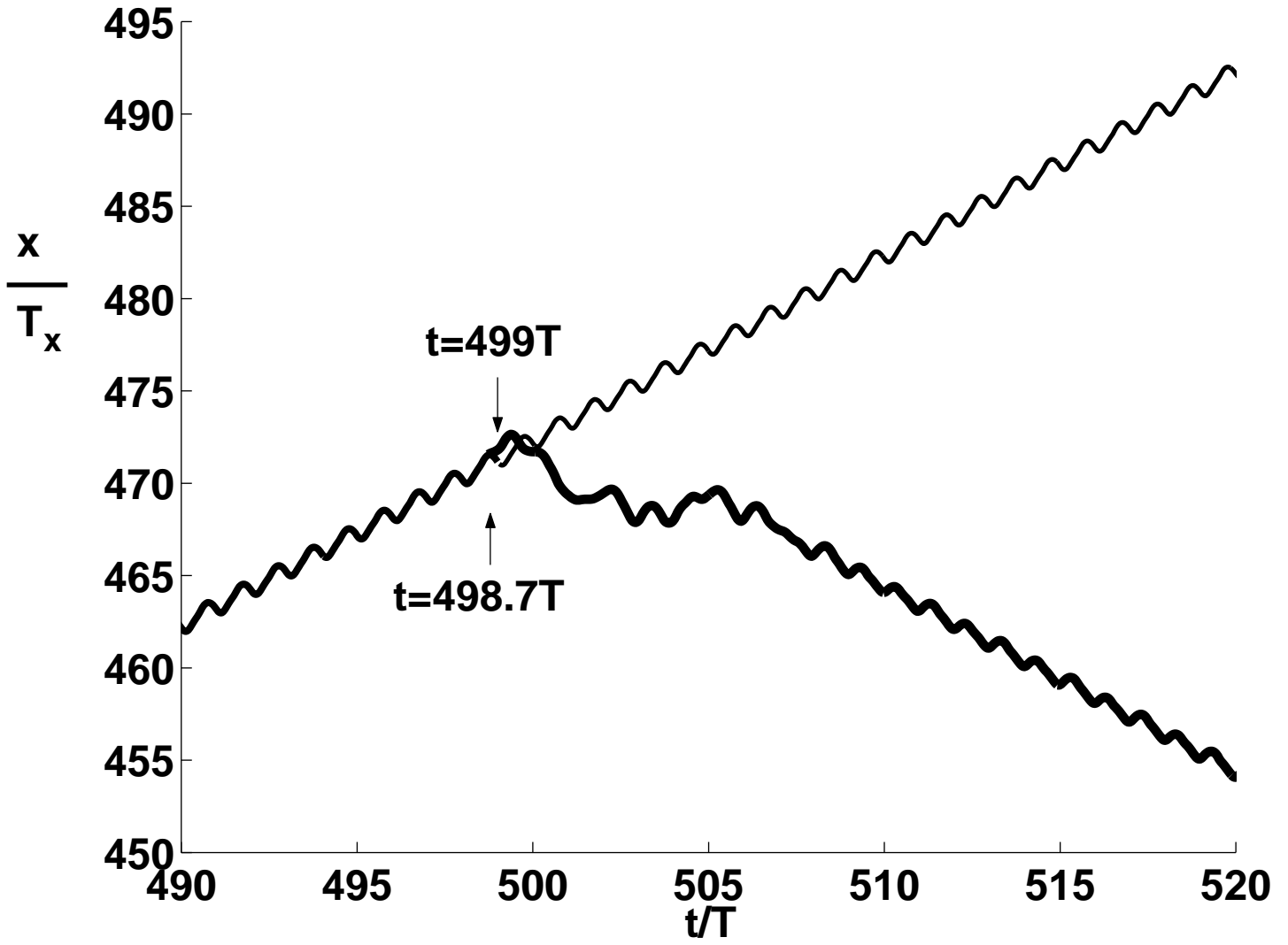


Fig. 8

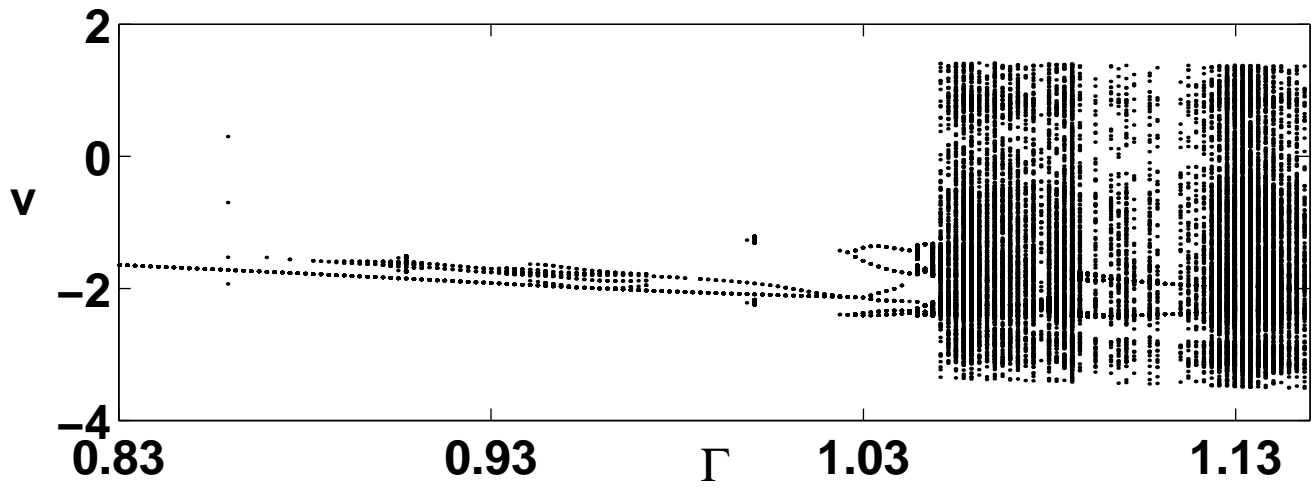
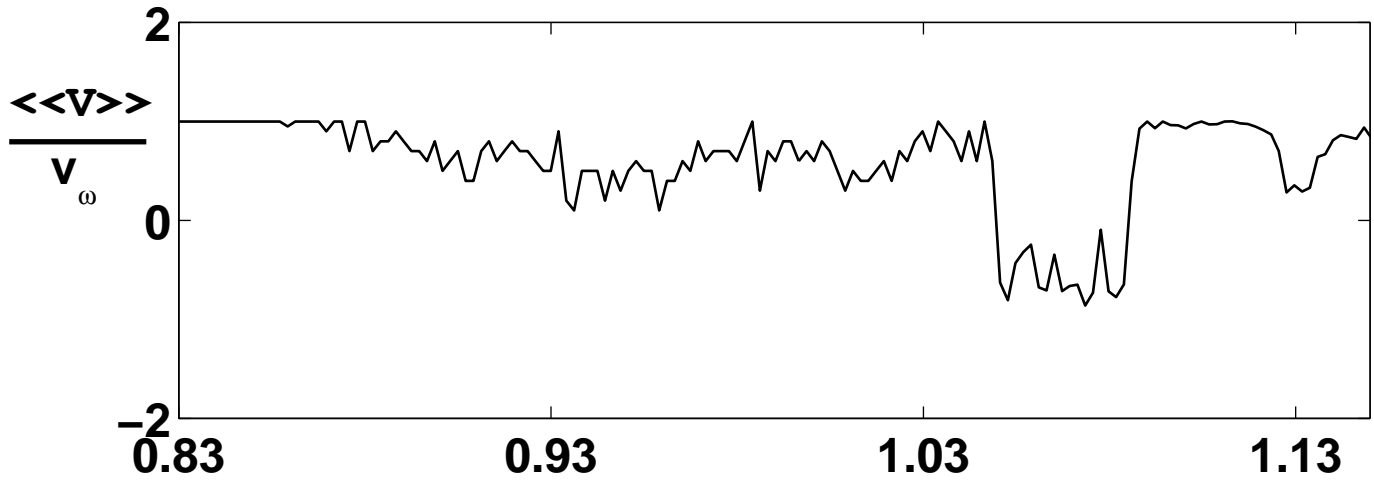


Fig. 9

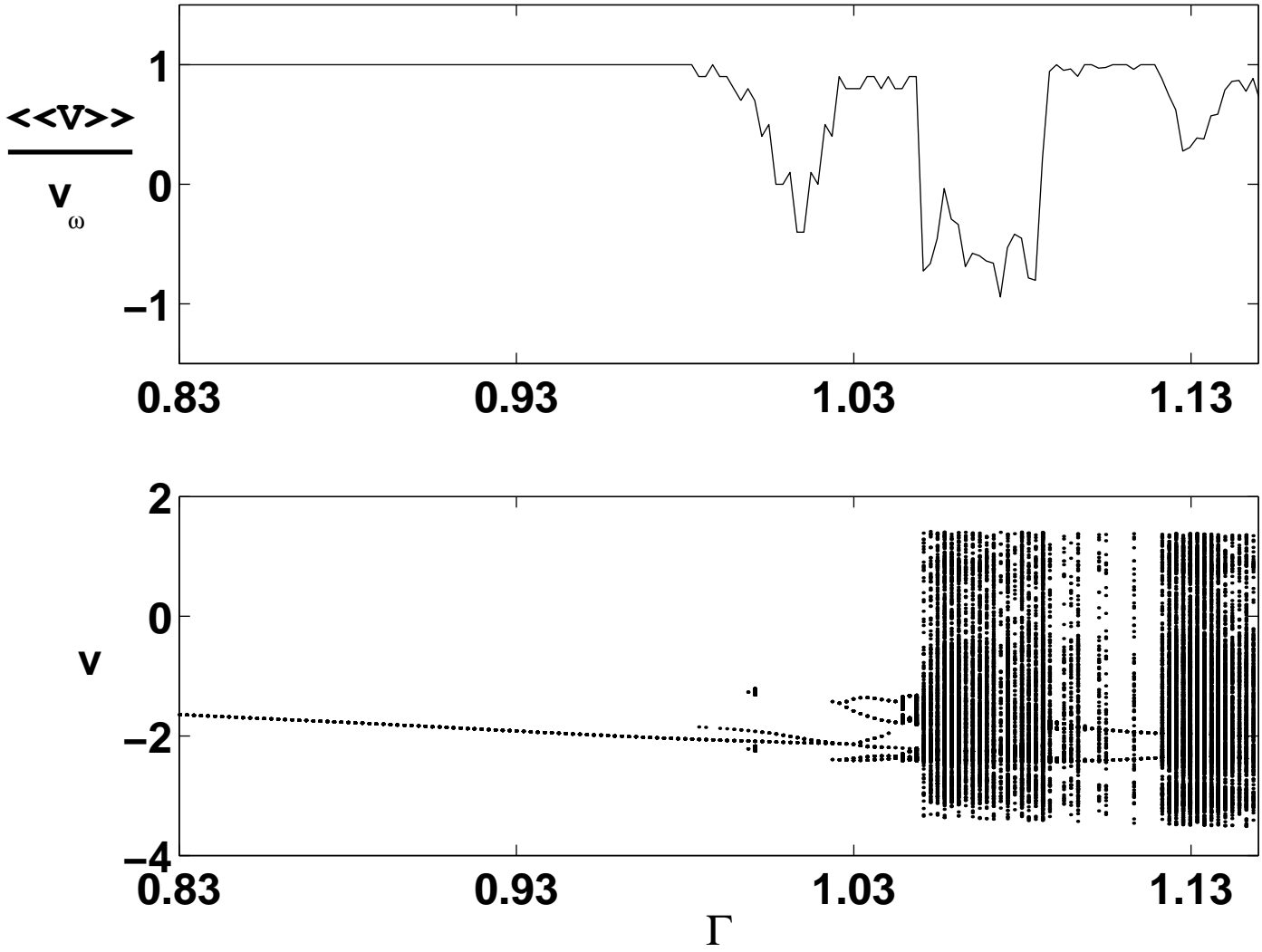


Fig. 10

